MIT Open Access Articles

Calcium Regulation of an Actin Spring

Massachusetts Institute of Technology

Calcium Regulation of an Actin Spring

Barney K. Tam,[†¶] Jennifer H. Shin,[∥] Emily Pfeiffer,[‡] P. Matsudaira,[‡§¶] and L. Mahadevan[††‡‡]*
[†]Department of Physics, [‡]Department of Biological Engineering, and [§]Department of Biology, Massachusetts Institute of Technology, Cambridge, Massachusetts 02139; [¶]Whitehead Institute for Biomedical Research, Cambridge, Massachusetts 02142; [∥]Department of Bio and Brain Engineering, and Department of Mechanical Engineering, KAIST, Daejeon, 305-701, Republic of Korea; [††]School of Engineering and Applied Sciences, and Department of Organismic and Evolutionary Biology, Harvard University, Cambridge, Massachusetts 02138; and [‡‡]Department of Systems Biology, Harvard Medical School, Boston, Massachusetts 02115

ABSTRACT   Calcium is essential for many biological processes involved in cellular motility. However, the pathway by which calcium influences motility, in processes such as muscle contraction and neuronal growth, is often indirect and complex. We establish a simple and direct mechanochemical link that shows how calcium quantitatively regulates the dynamics of a primitive motile system, the actin-based acrosomal bundle of horseshoe crab sperm. The extension of this bundle requires the continuous presence of external calcium. Furthermore, the extension rate increases with calcium concentration, but at a given concentration, we find that the volumetric rate of extension is constant. Our experiments and theory suggest that calcium sequentially binds to calmodulin molecules decorating the actin filaments. This binding leads to a collective wave of untwisting of the actin filaments that drives bundle extension.

INTRODUCTION

Calcium regulates the dynamics of many motile cellular processes. For example, calcium binding to the protein troponin C (1) mediates muscle contraction, whereas calcium concentration gradients (2) regulate neurite growth cone elongation. In *Vorticella*, calcium plays a direct role in neutralizing a charged polyeletrolyte gel that on contraction drives movement (3). In each of these systems, the mechanics of motility are coupled to the chemistry of calcium binding. Understanding this often complex coupling is an important problem in biology.

In this study, we establish a simple and direct mechanochemical link that shows how calcium quantitatively regulates the dynamics of a primitive motile system, the actin-based acrosomal process of the *Limulus* sperm. The acrosomal reaction of these cells is an example of micron-scale movement occurring in short (~10 s) timescales. During fertilization, a 60-μm long bundle of actin filaments, originally coiled within the cell (Fig. 1 *A*), straightens and extends to puncture protective layers covering the egg (4). This actin bundle is crystalline and tapered with a tip consisting of ~15 filaments, and a base of ~80 filaments (5). Each actin monomer is decorated in a 1:1 fashion by a scruin-calmodulin complex and neighboring filaments are bound to each other by scruin-scruin interactions (6,7). Scruin initially locks the actin filaments into a slightly overtwisted coiled superhelical bundled state, whereas calmodulin (CaM) confers calcium-sensitivity. On binding of calcium to CaM, the scruin-CaM complex unlatches, causing the filament—and hence bundle—overtwist to relax and drive the extension of this actin spring into the straight true discharge

(TD) state (6,8). Though the presence of external calcium is required for the reaction to occur, no quantitative experiments have investigated the role of calcium in the reaction. Specifically, it remains unclear whether calcium is required only to initiate the reaction, with the subsequent extension proceeding independently of calcium or if calcium is continuously required during the extension. To address this issue and probe the effects of external calcium on the dynamics of the TD extension, we use laser irradiation to trigger the TD reaction in a controlled environment, and use fluorescence to image calcium during the reaction.

MATERIALS AND METHODS

Sperm cells were collected from male crabs and washed in artificial sea water (ASW: 423 mM NaCl, 9 mM KCl, 9.27 mM CaCl$_2$, 22.94 mM MgCl$_2$, 25.5 mM MgSO$_4$, 2.15 mM NaHCO$_3$, 10 mM Tris, pH adjusted to 7.9–8.0) twice. The sample was then diluted 1:1000 with ASW and flowed into a flow chambers constructed from coverslips and double-sided adhesive tape to conduct the experiments. To immobilize the cells, the bottom coverslip was first treated with a 2% (v/v in acetone) BIOBOND nonspecific adhesive solution (BBInternational Inc., Cardiff, UK) and then rinsed with water.

An EGTA solution was prepared by substituting 0.1 mM EGTA for 9.27 mM CaCl$_2$ to chelate residual Ca^{2+} ions. Solutions for the calcium titration experiments were made by dissolving additional amounts of CaCl$_2$ to ASW as required to achieve desired calcium concentrations.

All experiments were carried out at room temperature with a Nikon TE-3000 inverted microscope with a NA 1.4 100× oil-immersion objective. A laser tweezer-like setup was installed with a 532-nm 25 mW laser from World Star Tech (Toronto, Ontario, Canada) to activate the cells. Video was recorded with a Dage MTI CCD100 camera, and digitized for tracking with a PC. Individual extension profiles were visually tracked using software provided by Photron Cameras (San Diego, CA).

RESULTS AND DISCUSSION

To find out if calcium is continuously required for the acrosomal reaction to proceed, we first trigger the TD reaction in ASW containing 9 mM CaCl$_2$ and simultaneously monitor
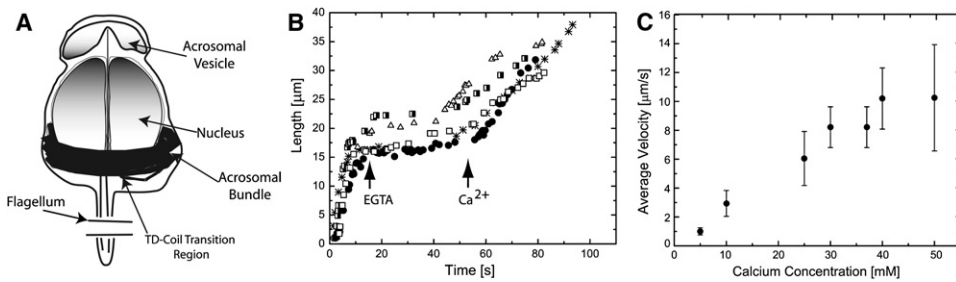

FIGURE 1 (A) Schematic of *Limulus* sperm cell. Note the gradual tapering of the bundle from the tip to the base (16–80 filaments), as well as the polygonal nature of the bundle itself. The region where a transition between the TD and coil occurs has a high degree of curvature in addition to a nonzero twist gradient, providing a possible location where calcium can preferentially bind to calmodulin. (B) Extension profile for multiple cells undergoing acrosome reaction. Arrows mark approximate introduction of EGTA, and at a later time, calcium-rich ASW. EGTA chelates calcium arresting the acrosome reaction. Reintroducing calcium restarts the extension. Such behavior is consistent with a reaction mechanism involving sequential binding of calcium to a local region on the bundle. (C) Effect of calcium on TD Extension. The average velocity of the TD extension increases at higher calcium concentrations. Each point averages over between 6 and 10 experiments.

the extension. As the actin bundle extends, we flow in a solution of zero-Ca^{2+} ASW with 0.1 mM EGTA, a calcium chelating agent that eliminates calcium. This has the effect of arresting

all motion within one second (Fig. 1 A). Reintroducing regular ASW to the flow chamber 30 s later results in a resumption of the extension, although with a lower velocity (Fig. 1 B).
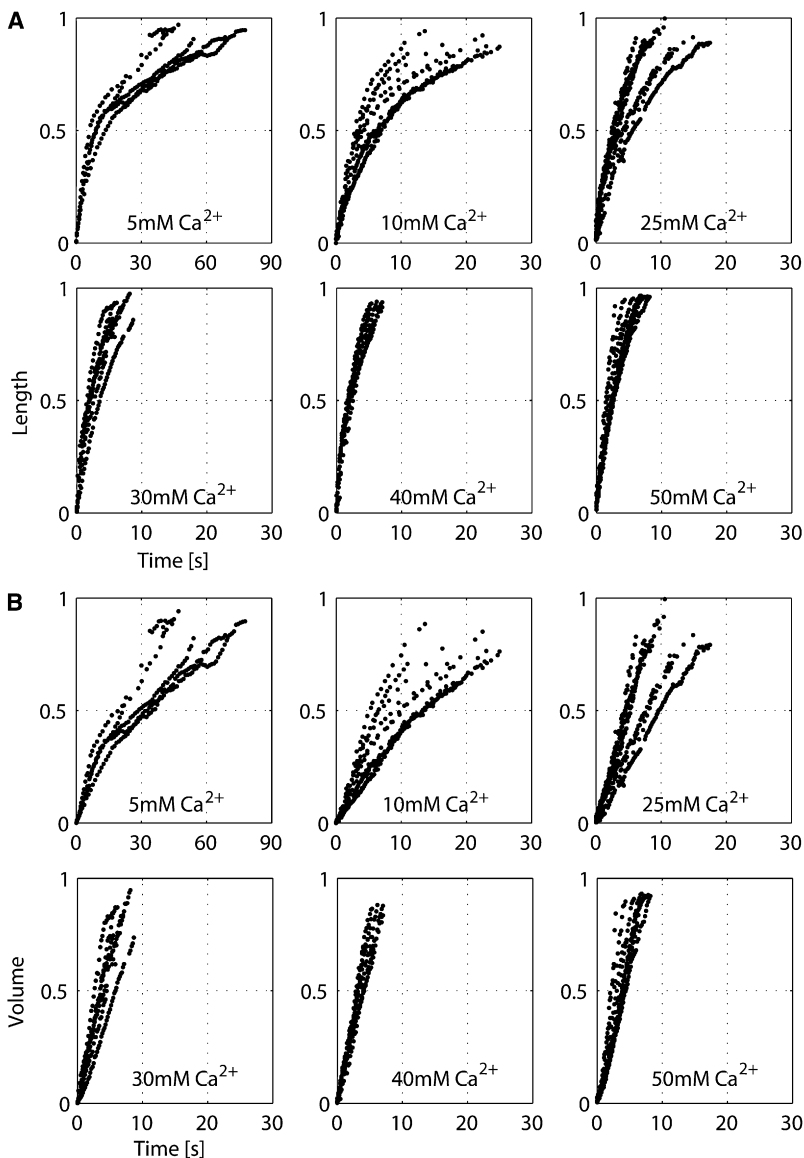
FIGURE 2 Series of calcium titration experiments measuring the TD extension. (A) The length of the bundle extends at an increasing rate as a function of calcium concentration but the trajectories exhibit significant nonlinear behavior at long times. (B) When the volume of the tapered bundle that is extended is plotted as a function of time, this nonlinearity is essentially eliminated for higher values of calcium concentration. However, for the low calcium (5, 10 mM) the nonlinearity and high variance data suggest stochastic binding behavior during CaM-Ca^{2+} reaction.

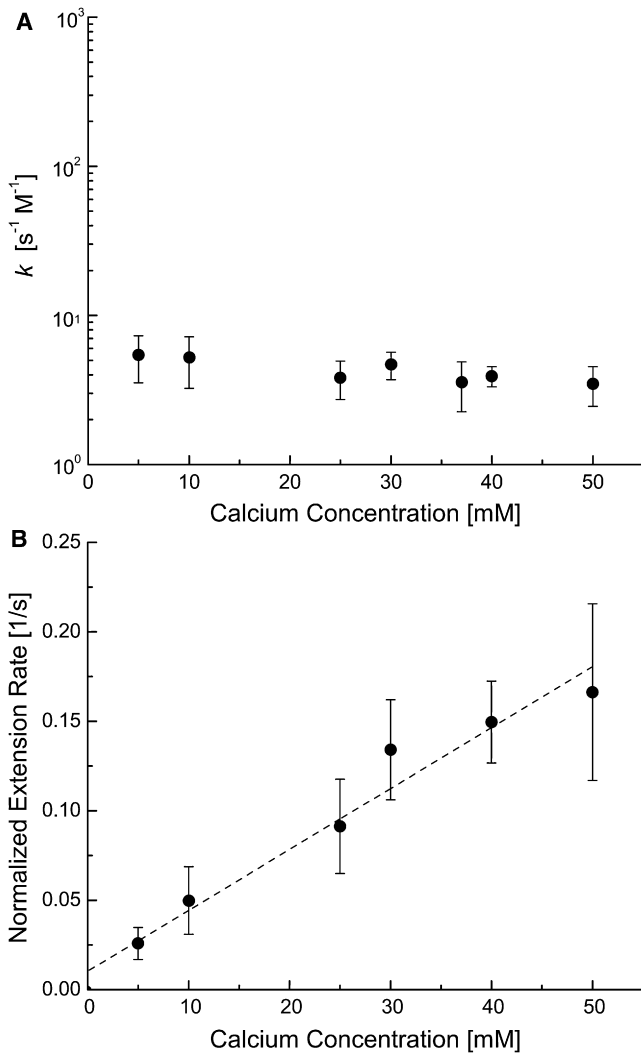FIGURE 3 (A) Rate constant k calculated using a noncooperative, constant rate CaM-Ca^{2+} binding mechanism. The slight dependence on $[Ca^{2+}]$ suggests a deviation from the mechanism due to an overestimation of [CaM] participating in the reaction. (B) Normalized volume extension rates. Values were calculated from least-squares fitting of volumetric extension profiles as functions of time. The linear behavior (*dashed line*) suggests a rate mechanism involving calmodulin with one calcium binding site.

As a control, we carried out a second series of experiments reversing the order of solutions added. Instead of ASW with calcium, we initially exposed the cells to zero-Ca^{2+} ASW solution and then irradiated the sperm with a laser. We find that the TD was never triggered in these experiments. However, when we replace the zero-Ca^{2+} solution with ASW within 15–20 s of laser irradiation, we are able to trigger the TD extension. Reintroducing ASW after a period >15–20 s does not produce TD extension. This probably occurs because although the laser induces depolarization of the membrane leading to the opening of voltage dependent calcium channels, its effect lasts only for a short time, after which the membrane becomes repolarized. Taken together, these experiments prove that the TD reaction proceeds only while the cell

is in calcium-rich ASW, eliminating the possible scenario where Ca^{2+} only initially triggers the extension, which then proceeds in a self-sustained manner. Moreover, the subsequent extension observed when calcium-rich ASW is reintroduced suggests that even though there is an abundance of calcium everywhere around the bundle (9), a localized untwisting mechanism generates motion, i.e., there is a localized front of filament and bundle untwisting along the bundle that propagates along it leading to extension.

To quantify the effect of external calcium concentrations on the dynamics of extension, we titrate the calcium concentrations in modified ASW to vary from 5 to 50 mM. In each solution of ASW, we trigger the acrosome reaction in different sperm cells, for a total of 6–10 sample extension profiles per concentration. Our results show that i), the velocity of extension increases as a function of calcium concentration (Fig. 1 C), and ii), the trajectories of all extensions exhibit significant nonlinear behavior (Fig. 2 A) at large extensions. The extension profiles of individual cells as a function of time show that the velocity of extension is not constant–it is initially large but decreases before the bundle is fully extended. To understand this, we begin with the simple fact that the bundle is tapered (3), so that the amount of actin, scruin, and calmodulin that are present in a stoichiometric ratio 1:1:1 varies with location along the bundle. Thus, consistent with a local mechanism for filament untwisting, the number of calmodulins available for binding is a function of the location and thus the length of the bundle that has untwisted. To quantify this dependence, we note that the volume of a tapered bundle of length L is given by $V = \int_0^L \pi r^2 dl$, where the radius $r = cl + r_0$. Integration yields $V(L) = \pi(c^2 \frac{L^3}{3} + cr_0 L^2 + r_0^2 L)$, where $c = 7.4 \times 10^{-4}$ and $r_0 = 24$ nm (10). Volume is hence a nonlinear function of the length, $L \in [0,60]$ μm. When we recast the bundle extension in terms of the volume extended as a function of time (Fig. 2 B), we find that the volume of the bundle extruded varies linearly with time. Moreover, the rate of this volume extension is dependent on the external calcium concentration, at least for low concentrations, but eventually saturates.

These observations can be understood by considering the binding of Ca^{2+} to the scruin-CaM complex, given by the following reaction mechanism:

$$CaM + Ca^{2+} \xrightarrow{k} CaM \cdot Ca^{2+}. \qquad (1)$$
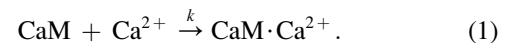
Here, k is an effective rate constant with units of $[M^{-1} \ s^{-1}]$, which governs the binding of Ca^{2+} to the scruin-CaM complex associated with the twisted filaments. We assume that unbinding occurs rarely so that we neglect its contribution to the kinetics. The local calcium concentration within the cell, $[Ca^{2+}]$, is essentially constant. This assumption is reasonable given that diffusion occurs on the order of milliseconds for a typical cellular dimension of 1 μm and a free diffusion coefficient $D = 140–300$ $\mu m^2/s$ for calcium ions in solution. We do not consider any Ca^{2+}-sequestering organelles or buffers (11,12). The concentration of calmodulin
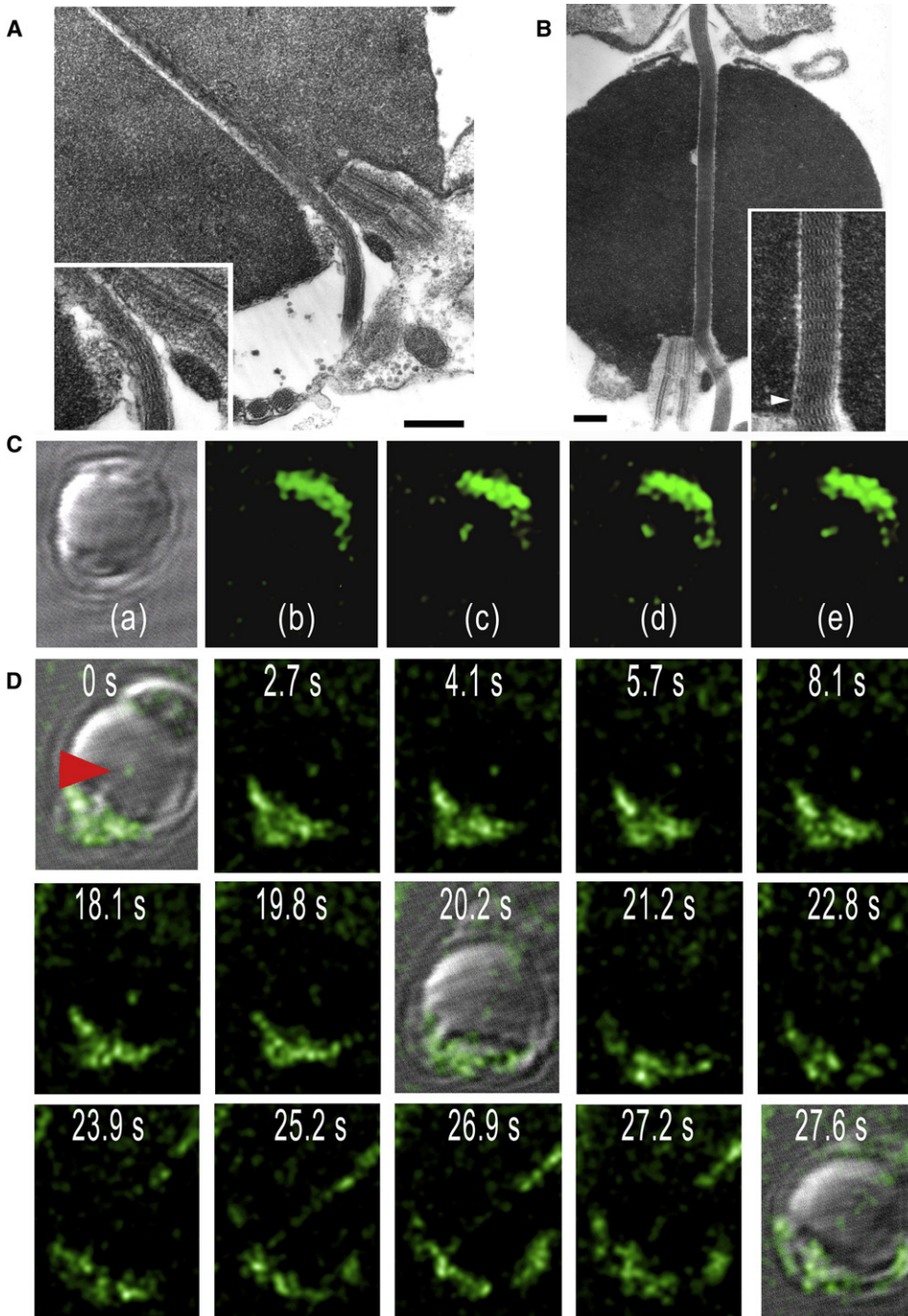
FIGURE 4 Entrance region of the nucleus before (*A*) and during (*B*) the extension. As evidenced in the electron micrographs, the bundle situated in the channel features an untwisted parallel array of filaments. This characteristic is typical of the true discharge bundle, whereas the part of the bundle entering into the channel is locally bent and twisted and exhibits slippage with respect to neighboring filaments (Scale bar, 100 nm). Filaments in the coil are twisted over each other at a regular interval and also have regularly spaced kinks (3). (*C*) Evidence for calcium localization during the acrosomal reaction. Selected frames showing calcium fluorescence from 2D time-lapse confocal microscopy using 7.7 mM of the AM-ester form of calcium green 1 for labeling. Image shown in (*a*) is a DIC image of an unreacted cell, (*b*) before, and (*c*, *d*, and *e*) 42, 47, and 50 s after the introduction of a calcium ion carrier (A23187) into the flow chamber. Once the ionophore is introduced into the flow chamber, a bright spot appears in the middle of the cell before the extension of the acrosome. (*D*) Images were captured immediately after calcium ionophore was added in the channel. Before the reaction begins (from 0 s to 18.1 s), calcium resides predominantly inside the cytoplasm at the base of the nucleus. A bright spot indicated by the arrowhead in the middle of the sperm head is also observed. As the extension begins (~after 10 s), this spot brightens briefly then disappears, whereas the extending bundle is brightly labeled with calcium dye indicating the association of calcium to the actin bundle. The bright spot, found in half of the collected data, is consistent with the presence of a localized region of calcium near the entrance region of the nuclear channel before extension. The extinction of this spot may be associated with the slight twitching of the sperm head typically observed during the bursting of the acrosomal vesicle at the beginning of extension.

participating in the reaction is constant for a given region and can be equated to the number density, n, of CaM in the bundle. To calculate this density, we again appeal to the bundle geometry. Because the helical pitch between adjacent actin monomers in the axial direction is 2.7 nm (3), 1 μm of this filament contains ~370 actin/scruin/CaM complexes. Because the 60-μm bundle tapers from 80 to 20 filaments, having an average 50 filaments, we calculate the total number of CaM to be ~1.13×10^6 (10). Using a total bundle volume, V_{tot}, of 2.0×10^{-19} m^3, calculated based on the measured dimensions of

a truncated cone (upper base radius, 10 nm; lower base radius, 50 nm; height, 60 μm), we thus find the number density n to be ~0.5×10^{-25} CaM mol/m^3, or equivalently, 8×10^{-3} M. On calcium binding, the CaM $\cdot$ Ca^{2+} complex allows the strained actin filaments to untwist, hence extending the kinked twisted bundle. The rate equation that quantifies this simple binding mechanism is

$$\frac{d[\text{CaM} \cdot \text{Ca}^{2+}]}{dt} = -\frac{d[\text{CaM}(L)]}{dt} = kn[\text{Ca}^{2+}]. \quad (2)$$

Given a constant $[Ca^{2+}]$, Eq. 2 trivially yields $[CaM \cdot Ca^{2+}] = kn[Ca^{2+}]t$. Because $CaM \cdot Ca^{2+}$ can only form on the bundle, the total number of complexes is $[CaM \cdot Ca^{2+}]V_{tot}$. However, the total number of $CaM \cdot Ca^{2+}$ complexes associated with a given volume, $V(L)$ of the extending bundle is $[CaM]V(L)$. These two quantities are equal to each other because the extension is a direct result of $CaM \cdot Ca^{2+}$ formation. This equality relates the kinetics associated with the Ca^{2+}-CaM reaction mechanism to the trajectories in Fig. 2 B for the volumetric extension rate. By identifying $V(L)/V_{tot} = knt[Ca^{2+}]/[CaM]$ as the effective volumetric reaction rate, and determining the rate constant, k, we find that it is independent of calcium concentration (Fig. 3 A), consistent with a single-site binding mechanism. Moreover, this binding rate is comparable to rate constants observed in other calcium binding systems (13,14).

Although a noncooperative two-site binding framework was used previously to analyze in vitro calorimetric experiments (9), our in vivo results suggest that CaM conformational change occurs with the binding of a single calcium ion. Purified bundles of actin, scruin, and CaM will most likely behave differently than bundles in a living cell. Conformation changes for the bundle in our experiments occur dynamically, far away from binding equilibrium, unlike the calorimetric experiments. Indeed, a characteristic rate of conformational change for CaM associated with the effective rate constant $k = 4 \, M^{-1}s^{-1}$ (Fig. 3 A) can be calculated by multiplying k by the saturating Ca^{2+} concentration of ~50 mM, yielding a value of $0.2 \, s^{-1}$. This value is significantly less than the observed closed $\rightarrow$ open rate of $2.7 \times 10^4 \, s^{-1}$ for CaM conformational changes (15), suggesting that calcium binding is not the rate-limiting step of the reaction. Instead, local rearrangements of the actin filaments as they slide relative to each other during untwisting are a much more likely candidate limiting the rate of extension. Such a mechanism can arise from the densely packed filamentous bundle, where the untwisting motions driven by calcium binding will lead to large local shear rates. In addition, this sequential binding mechanism suggests that the highly strained transition region characterizing the TD-coil interface as it bends/twists into the nuclear channel is where calcium ions preferentially bind to CaM. This follows because a highly strained region allows significantly greater access to the Ca^{2+} binding sites of CaM, hence facilitating the reaction and increasing the rate of calcium binding locally. Indeed, in Fig. 4, A and B, we show electron micrographs consistent with this structural transition region of the bundle near the entrance to the nuclear channel.

To complement the kinetic measurements, we also used calcium imaging via fluorescence to follow the acrosomal reaction in time. In Fig. 4, C and D, we show the results of 2D time-lapse confocal microscopy to track the dynamics of calcium introduced using an ionophore. We see that before the reaction starts, the calcium resides inside the cytoplasm at the base of the nucleus. On activation however, the extending bundle is labeled with the calcium dye, which is consistent with the association of calcium with the bundle. In addition, a bright spot is observed in half of the images near the entrance of the bundle into the channel (Fig. 4 A), implying that calcium binds at a localized region.

Our experiments are consistent with a model that accommodates a sequential calmodulin-calcium binding mechanism and that presents a natural region within the bundle wherein the reaction occurs. Knowledge of how calcium binds to calmodulin (13), and of the structural transformations of the actin bundle (16) provides us with a biophysical basis that combines structural and dynamical information to show the mechanochemistry of a simple actin spring that stores energy and, when activated, generates force (9,17) to carry out a crucial physiological function.

REFERENCES

1. Farah, C. S., and F. C. Reinach. 1995. The troponin complex and regulation of muscle contraction. *FASEB J.* 9:755–767.

2. Henley, J., and M. Poo. 2004. Guiding neuronal growth cones using Ca^{++} signals. *Trends Cell Biol.* 14:320–330.

3. Katoh, K., and M. Kikuyama. 1997. An all-or-nothing rise in cytosolic $[Ca^{++}]$ in *Vorticella sp. J. Exp. Biol.* 200:35–40.

4. Brown, G. G., and W. J. Humphreys. 1971. Sperm-egg interactions of *Limulus polyphemus* with scanning electron microscopy. *J. Cell Biol.* 51:904–907.

5. Tilney, L. G. 1975. Actin filaments in the acrosomal reaction of *Limulus* sperm. *J. Cell Biol.* 64:289–310.

6. Sanders, M. C., M. Way, J. Sakai, and P. Matsudaira. 1996. Characterization of the actin cross-linking properties of the scruin-calmodulin complex from the acrosomal process of *Limulus* sperm. *J. Biol. Chem.* 271:2651–2657.

7. Shin, J. H., M. L. Gardel, L. Mahadevan, P. Matsudaira, and D. A. Weitz. 2004. Relating microstructure to rheology of a bundled and cross-linked F-actin network in vitro. *Proc. Natl. Acad. Sci. USA.* 101:9636–9641.

8. DeRosier, D. J., L. G. Tilney, E. M. Bonder, and P. Frankl. 1982. A change in twist of actin provides the force for the extension of the acrosomal process in *Limulus* sperm. *J. Cell Biol.* 93:324–337.

9. Shin, J. H., L. Mahadevan, G. S. Waller, K. Langsetmo, and P. Matsudaira. 2003. Stored elastic energy powers the 60μm extension of the *Limulus polyphemus* sperm actin bundle. *J. Cell Biol.* 162:1183–1188.

10. Shin, J. H., L. Mahadevan, P. T. So, and P. Matsudaira. 2004. Bending stiffness of a crystalline actin bundle. *J. Mol. Biol.* 337:255–261.

11. Allbritton, N. L., T. Meyer, and L. Stryer. 1992. Range of messenger action of calcium ion and inositol 1,4,5-trisphosphate. *Science.* 258:1812–1818.

12. Al-Baldawi, N. F., and R. F. Abercrombie. 1995. Calcium diffusion coefficient in *Myxicola* axoplasm. *Cell Calcium.* 17:422–430.

13. Chin, D., and A. R. Means. 2000. Calmodulin: a prototypical calcium sensor. *Trends Cell Biol.* 10:323–328.

14. Dong, W. J., C. K. Wang, A. M. Gordon, S. S. Rosenfeld, and H. C. Cheung. 1997. A kinetic model for the binding of Ca^{2+} to the regulatory site of troponin from cardiac muscle. *J. Biol. Chem.* 272:19229–19235.

15. Evenas, J., J. Malmendal, and M. Akke. 2001. Dynamics of the transition between open and closed conformations in a calmodulin C-terminal domain mutant. *Structure.* 9:185–195.

16. Schmid, M. F., M. B. Sherman, P. Matsudaira, and W. Chiu. 2004. Structure of the acrosomal bundle. *Nature.* 431:104–107.

17. Shin, J. H., B. K. Tam, R. R. Brau, M. J. Lang, L. Mahadevan, et al. 2007. Force of an actin spring. *Biophys. J.* 92:1–5.